

Raman scattering from sp^2 carbon clusters

M. Yoshikawa, N. Nagai, M. Matsuki, H. Fukuda, G. Katagiri, H. Ishida, and
A. Ishitani

Toray Research Center, Inc., Sonoyama 3-3-7, Otsu, Shiga 520, Japan

I. Nagai*

Research Development Corporation of Japan, Kuroda Solid Surface Project, Sonoyama 3-3-7, Otsu, Shiga 520, Japan

(Received 12 July 1991; revised manuscript received 4 May 1992)

Raman spectra of B ion-implanted glassy carbon (GC) and hydrogenated amorphous carbon (a -C:H) films have been measured as a function of polarization direction of the scattered light and excitation wavelength. Raman bands of GC implanted heavily with a fluence of more than 5×10^{15} B ions/cm² and a -C:H films show a frequency-independent depolarization ratio, suggesting the existence of sp^2 carbon clusters in these samples. It was found that Raman spectra of GC implanted heavily with a fluence of more than 5×10^{15} B ions/cm² varied with the excitation wavelength. From a comparative study of the heavily implanted GC and a -C:H films, the variation of the Raman spectra with the excitation wavelength observed for the heavily implanted GC is interpreted in terms of π - π^* resonant Raman scattering from sp^2 carbon clusters having various sizes.

I. INTRODUCTION

To date, several workers have measured the Raman spectra of graphite. The highly oriented pyrolytic graphite (HOPG) is mostly aligned along the c axis, but in the layered planes it consists of a randomly ordered collection of crystallites having a 1- μ m average diameter. A Raman band assigned to the C=C stretching vibration E_{2g} mode is observed at 1581 cm⁻¹ in the HOPG.¹ The peak frequency of the E_{2g} mode shifts to a higher frequency with the decrease in the crystallite size of the graphite layers. In glassy carbon (GC) having a crystallite size of ~ 25 Å, the E_{2g} mode is observed at 1590 cm⁻¹. Furthermore, an additional band appears around 1355 cm⁻¹ with the decrease of crystallite size in the graphitic layers. The 1355-cm⁻¹ band, called the disorder mode, is assigned to the A_{1g} -type mode at the K point of the Brillouin zone activated by the disorder.² Generally, in amorphous materials, the observed Raman spectrum reflects the vibrational density of states, which is similar to that of the crystal.³ There are two maxima, one at 1355 cm⁻¹ near the K point of the Brillouin zone, the other at 1590 cm⁻¹ in the calculated density state of graphite. The Raman spectrum of GC can be explained by the vibrational density of states in the graphite.

Hydrogenated amorphous carbon (a -C:H) films have been confirmed to consist of a mixture of tetrahedral (sp^3) and trigonal (sp^2) bonding structures, based on the results from a number of analytical techniques including Raman spectroscopy.⁴⁻¹³ We have measured Raman spectra of a -C:H films prepared by chemical-vapor-deposition (CVD) and sputtering methods.^{5,6} Raman spectra of a -C:H films consist of a broad band centered around 1550 cm⁻¹ and a shoulder band near 1400 cm⁻¹. The Raman spectral profiles have been found to vary with the excitation wavelength, depending on the electronic absorption spectra associated with π - π^* electronic transitions.⁵⁻⁷

This spectral variation with excitation wavelength for a -C:H films is very similar to that for the disorder mode in GC.⁸ The dependence of Raman spectra on the wavelength of the excitation is interpreted in terms of π - π^* resonant Raman scattering from sp^2 carbon clusters with various sizes. Considering that the Raman-scattering cross section of diamond (9.1×10^{-7} cm⁻¹ sr⁻¹) is much lower than that of graphite (5×10^{-5} cm⁻¹ sr⁻¹),¹⁴ we have concluded that the π - π^* resonant Raman scattering from various-sized sp^2 carbon clusters is dominant in the spectra of the visible region between 4579 and 6471 Å.^{5,6,8}

Recently, Wagner *et al.* have measured Raman spectra of amorphous carbon films.⁹ They divided the Raman spectra of the amorphous carbon films into two phases. Phase 1, between 1400 and 1550 cm⁻¹, was assigned to the vibration due to sp^3 carbon clusters resulting from an enhancement of phase 1 at 4.8 eV near the σ - σ^* transition energy of sp^3 carbon. Phase 2, at 1600 cm⁻¹, was assigned to the vibration due to sp^2 carbon clusters. Their assignment for phase 1 is different from our interpretation that phase 1 is due to the sp^2 carbon clusters. The measurement on the polarization property for phases 1 and 2 can give some information about the origin of the Raman bands in the amorphous carbon films.

Robertson and O'Reilly have calculated the electronic structures of a -C:H films and asserted that such films having an optical gap of 1.5 eV contain sp^2 carbon clusters with a crystallite diameter size of ~ 15 Å.¹⁵ In GC having a crystallite size of ~ 25 Å, two Raman bands are observed at 1355 and 1590 cm⁻¹. If Raman bands of a -C:H films originate from sp^2 carbon clusters, the profile and polarization property of the Raman spectrum for the GC should approach those for a -C:H films with a decrease of crystallite size by ion implantation. Furthermore, π - π^* resonant Raman scattering from sp^2 carbon clusters observed for a -C:H films can also occur in ion-

implanted GC. In the present work, the microstructures of the heavily implanted GC and *a*-C:H films will be discussed based upon the Raman spectral variations with polarization direction of the scattered light and excitation wavelength.

II. EXPERIMENT

HOPG and PG crystal plates from the Union Carbide Corporation, and GC crystal plates from the Tokai Carbon Corporation, were used in the present work. The HOPG plates were heat treated at 3000°C under a compressive stress parallel to the average direction of the *c* axis. PG and GC plates were heat treated at 1500 and 2000°C, respectively. The GC was implanted at 60 keV with a fluence of 1×10^{15} – 1×10^{16} B ions/cm².

The *a*-C:H films were prepared on Si and glass substrates from CH₄ gas by an electron-cyclotron-resonance plasma, chemical-vapor-deposition (ECR-P-CVD) method. Several samples labeled from *A* to *C* were prepared by changing the substrate temperature over the range of 150–250°C. The total pressure was kept constant at approximately 10^{-5} Torr.

Raman spectra were measured at room temperature with several lines of argon- and krypton-ion lasers. Polarized and depolarized Raman spectra were measured in backscattering and 90° scattering geometries, respectively, and recorded at a low power of 40–60 mW to avoid any thermal decomposition of the samples. Raman spectra were recorded with use of a Jobin Yvon Ramanor U-1000 double monochromator, equipped with a photomultiplier and photon-counting electronics.

III. RESULTS AND DISCUSSION

A. The depolarization ratio for B ion-implanted GC and *a*-C:H film

Figure 1 shows Raman spectra of GC, B ion-implanted GC crystals, and *a*-C:H film. In the GC, two Raman bands are observed at 1355 and 1590 cm⁻¹. The crystallite size of GC is estimated to be ~ 25 Å from the relative intensity between 1355 and 1590 cm⁻¹ bands, as is well known from Ref. 2. As can be seen, the position of the *E*_{2g} mode at 1590 cm⁻¹ shifts toward lower frequency, whereas the position of the disorder mode shifts to a higher frequency with an increase of B ion implantation. The Raman spectral variation of GC crystals with B ion implantation bears a resemblance to the results reported by Elman.¹⁶ An asymmetric broad band is observed around 1550 cm⁻¹ in the spectra of the GC implanted with a fluence of 1×10^{16} B ions/cm². The Raman spectral profile of this heavily implanted GC is similar to that of the *a*-C:H film.

Raman spectra of several samples were measured with two different geometries; one with both the incident light polarized and the scattered light analyzed perpendicular to the scattering plane (\parallel), the other with the incident light polarized perpendicular to and the scattered light analyzed parallel to the scattering plane (\perp). Figure 2 shows Raman spectra of the HOPG, PG, GC, B ion-implanted GC and *a*-C:H film measured with these

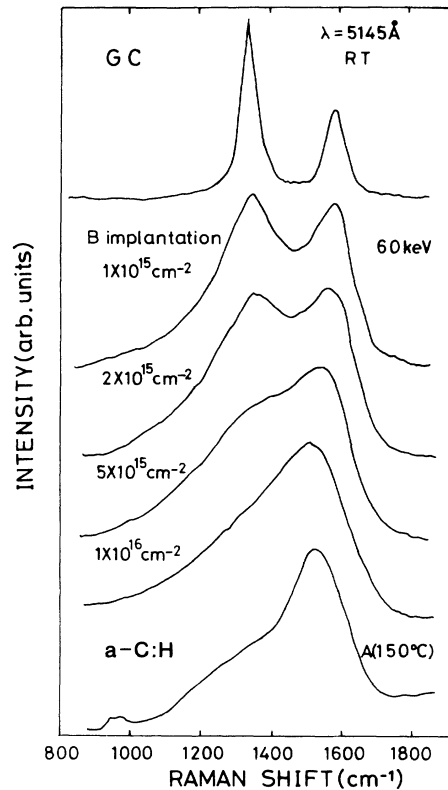


FIG. 1. The Raman spectra of GC, GC implanted with various fluences, and *a*-C:H film prepared at 150°C.

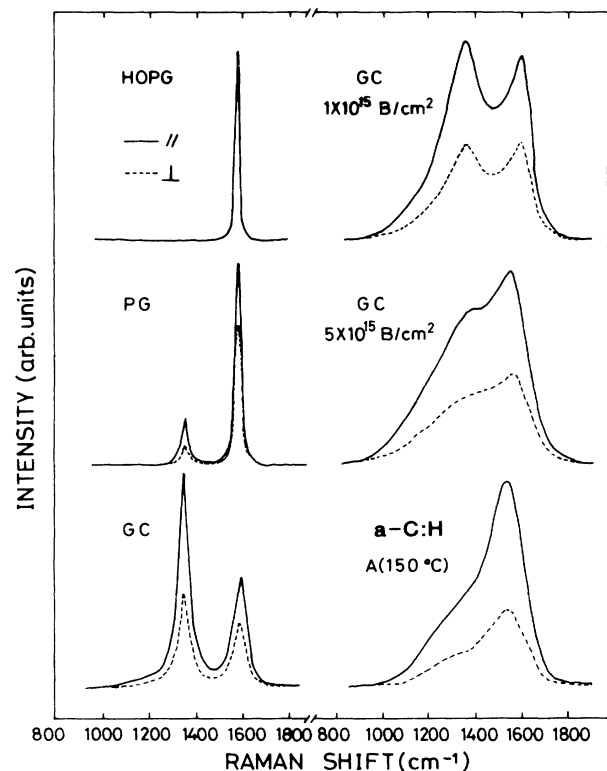


FIG. 2. Polarized Raman spectra of HOPG, PG, GC, and B ion-implanted GC, and *a*-C:H film.

geometries. When the Raman spectra were taken in a backscattering geometry, the polarization vectors of incident and scattered light lie in the sample plane.

The Raman tensors for the E_{2g} mode of graphite, R_j ($j = 1, 2$), are given by^{14,17}

$$\begin{pmatrix} 0 & d & 0 \\ d & 0 & 0 \\ 0 & 0 & 0 \end{pmatrix}$$

and

$$\begin{pmatrix} d & 0 & 0 \\ 0 & -d & 0 \\ 0 & 0 & 0 \end{pmatrix}.$$

The Raman-scattering intensity is generally expressed as¹⁷

$$I \sim \sum_j (e_i R_j e_s)^2, \quad (1)$$

where e_i and e_s are the unit polarization vectors of incident and scattered light, respectively. From Eq. (1), the depolarization ratio, $D_p = I_{\perp}/I_{\parallel}$ for the E_{2g} mode is expressed as $D_p = 1$ for crystal and $3/4$ for polycrystal.

Figure 3 shows the relationship between the peak frequency and D_p for the E_{2g} mode and the disorder mode. Raman spectra were decomposed into two bands with Lorentzian or Gaussian line shapes. Raman spectra of

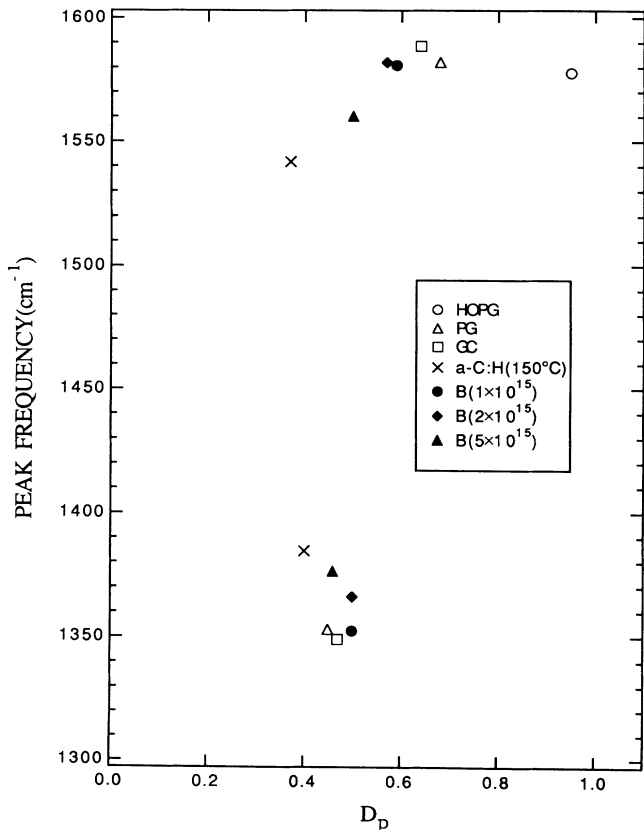


FIG. 3. The relationship between the peak frequency and the depolarization ratio, $D_p = I_{\perp}/I_{\parallel}$.

a -C:H films can be well resolved to two bands with Gaussian line shapes.^{5,6,8} The measured values of D_p were calibrated against reference peaks of carbon tetrachloride, whose 218- and 314- cm^{-1} bands are known to be completely depolarized ($D_p = 0.75$).¹⁸ As seen in Fig. 3, the observed D_p of the E_{2g} mode for HOPG is about unique, being in agreement with the value expected from Eq. (2). The D_p for the E_{2g} mode decreases from ~ 1.0 to 0.64 with the decrease in the crystallite size of the graphitic plane, ranging from the HOPG to GC. In the B ion-implanted GC, D_p for the E_{2g} mode decreases to 0.50 with an increase of the ion implantation. The experimental values of D_p for the B ion-implanted GC are much lower than the value for the polycrystal (0.75). This low D_p value implies that the high-frequency band observed in the B ion-implanted GC no longer conserve the E_{2g} symmetry, suggesting that each crystallite is broken by the ion implantation and converted into small sp^2 clusters. The breakdown of F_{2g} symmetry for the F_{2g} mode has been observed in small silicon particles with an average particle size from 60 to 350 Å.¹⁹

Dillon, Woollam, and Katkanant²⁰ have measured Raman spectra of carbon films prepared by ion-beam and rf-discharge deposition as a function of anneal temperature, and pointed out that the positions of E_{2g} and disorder modes shift to high frequency with the removal of the disorder.²⁰ The downshift of the E_{2g} mode with the increase of the ion implantation for the ion-implanted GC is consistent with their result, whereas the upward shift of the disorder mode seems to disagree with their result. We believe that this disagreement originates from an uncertainty of the peak frequency obtained from the Lorentzian fit to the weak broadband measured by Dillon, Woollam, and Katkanant.

D_p values for the disorder mode vary from 0.45 to 0.50. With an increase of the ion implantation, the peak frequencies of the disorder mode and E_{2g} mode approach each other, and the D_p values for the disorder mode and the E_{2g} mode also tend to approach each other. The D_p values for GC implanted heavily with a fluence of more than 5×10^{15} B ions/ cm^2 are almost independent of the phonon frequency.

The polarization properties of the Raman spectra have been used to test the validity of two structural models of amorphous materials, a random-network model and a molecular one. Iqbal and Vepřek²¹ have summarized the properties of D_p as follows: In a continuous random network (CRN) model, D_p should be frequency dependent because all vibrational modes with different local symmetry characters contribute to the scattering. In the case of the molecularlike cluster model, D_p is frequency independent and $D_p \rightarrow 0$ in the ideal case of no intercluster interaction, but has a high value in the condensed case. The frequency-independent D_p value for the heavily implanted GC confirms the existence of sp^2 carbon clusters in the heavily implanted GC.

The D_p value of the high-frequency band for the a -C:H film was found to be 0.37 and independent of the phonon frequency, being nearly in agreement with that of the shoulder band near 1400 cm^{-1} . The D_p values of Raman

bands for the *a*-C:H film are close to those for the heavily implanted GC. From the similarity between the Raman spectra of *a*-C:H films and heavily implanted GC, and from the comparison between their Raman band polarization properties, the two Raman bands observed in the *a*-C:H films are considered to originate from the sp^2 carbon clusters.

As can be seen in Fig. 3, the D_p values for the ion-implanted GC tend to decrease with an increase of the ion implantation. Tamor *et al.* studied changes in the relative intensity between 1355 and 1590 cm^{-1} in *a*-C:H films as a function of bias voltage.^{22,23} According to their data, the relative intensity increases with the decrease of sp^2 crystallite size, L_a , showing a maximum near $L_a = 12$ Å and then a decrease as L_a decreases. In the spectra of GC and the ion-implanted GC with the \parallel configuration, the relative intensity varies from 1.8 to 3.9 as the fluence increases from 0 to 5×10^{15} B ions/ cm^2 . Referring to their result, L_a for the ion-implanted GC decreases from ~ 25 to ~ 12 Å with the ion implantation. Since the D_p value in the molecularlike cluster model is expected to decrease with a decrease of L_a because of a decrease of the intercluster interaction,²¹ the decreasing tendency of the D_p values with decreasing L_a for the ion-implanted GC can be well explained by the molecularlike cluster model.

Lannin and Li have recently measured the radial distribution function of the sputtered amorphous carbon (*a*-C) film.²⁴ Based upon the absence of a 2.84-Å third-nearest-neighbor peak due to cross-ring distances, they have deduced that the sputtered *a*-C film is composed of a graphitic random network. Their interpretation for the sputtered *a*-C film seems to be inconsistent with our interpretation for the *a*-C:H films. The sputtered *a*-C film shows Raman spectra consisting of the main peak at 1560–1580 cm^{-1} and the disorder mode around 1400 cm^{-1} . The intensity of the disorder mode for the sputtered *a*-C films is generally stronger than that for the *a*-C:H films, showing that the crystallite size of the sputtered *a*-C films is larger than that of the *a*-C:H films.²⁵ Hence, we believe that the difference between our interpretation and their interpretation originates from a difference between microstructures of the sputtered *a*-C and *a*-C:H films. The measurement of the frequency dependence of the depolarization ratio, the depolarization spectrum, may give detailed information about the microstructures of *a*-C or *a*-C:H films.

B. Resonant Raman scattering from sp^2 carbon clusters

Figures 4 and 5 show Raman spectra of the GC crystal, the B ion-implanted GC, and *a*-C:H film obtained with various excitation wavelengths. The positions of the E_{2g} modes for the GC and GC implanted with a fluence of 2×10^{15} B ions/ cm^2 hardly depend on excitation wavelength. However, the position of the disorder mode shifts to lower frequency with an increase in excitation wavelength. In the GC implanted heavily with fluences greater than 5×10^{15} B ions/ cm^2 , the position of the E_{2g} mode begins to shift toward lower frequency as the exci-

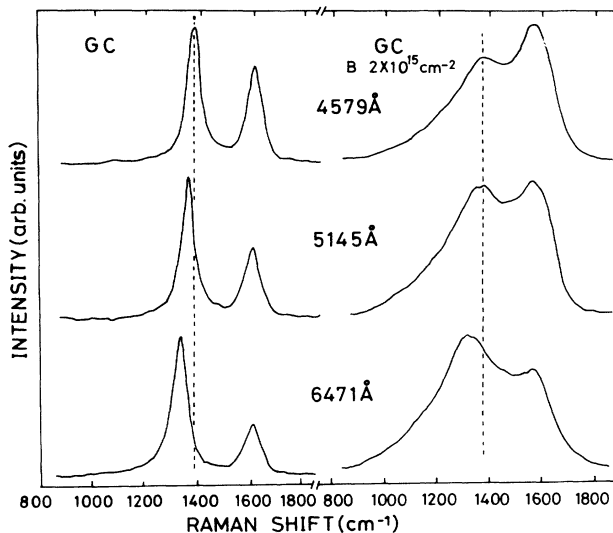


FIG. 4. The Raman spectra of GC and GC implanted with a fluence of 2×10^{15} B ions/ cm^2 obtained with various excitation wavelengths.

tation wavelength increases. The position of the main peak around 1550 cm^{-1} for the *a*-C:H film prepared at 150°C also shifts to lower frequency as the excitation wavelength increases. The variation in the Raman spectra of the *a*-C:H film as the excitation wavelength increases agrees well with that of GC implanted with a fluence of 1×10^{16} B ions/ cm^2 .

The dependence of the peak frequencies on the wavelength of the excitation light for the two decomposed Raman bands is plotted in Fig. 6. As the ion implantation increases, the position of the E_{2g} mode shifts toward lower frequency with an increase in the excitation wavelength. The dependence of the frequencies of the two decomposed Raman bands on the excitation wavelength for GC implanted with a fluence of 1×10^{16} B ions/ cm^2 coincides well with that of the disorder mode in GC, and

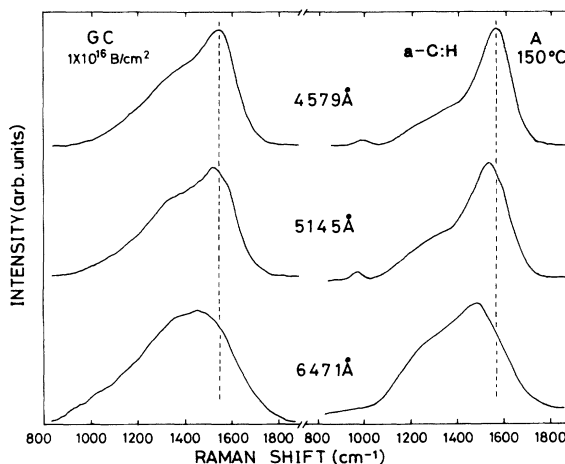


FIG. 5. The Raman spectra of GC implanted with a fluence of 1×10^{16} B ions/ cm^2 and *a*-C:H film prepared at 150°C with various excitation wavelengths.

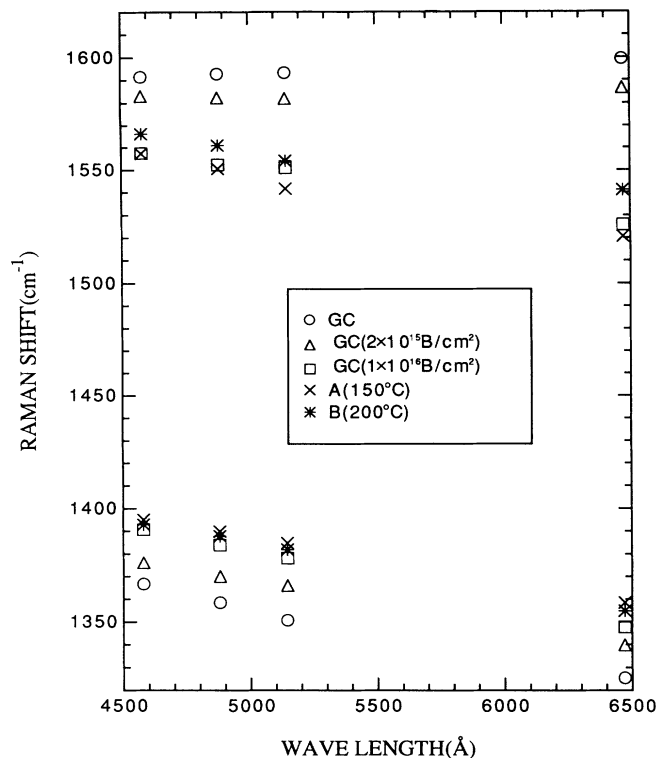


FIG. 6. The dependence of the peak frequencies on the excitation wavelength for GC, the B ion-implanted GC, and a -C:H films. Raman spectra are decomposed into two bands with Lorentzian or Gaussian line shapes. The frequencies of the two decomposed Raman bands are plotted in Fig. 6.

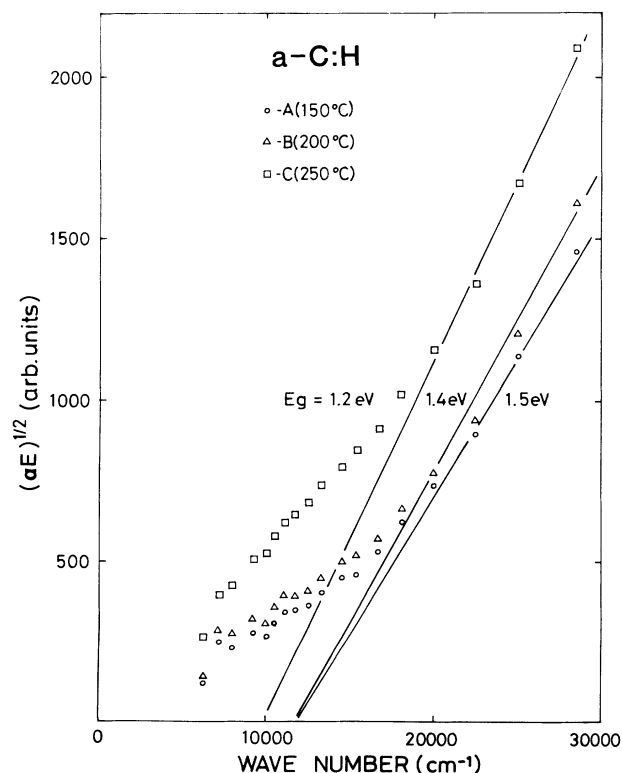


FIG. 7. Optical gap behavior of a -C:H films prepared at various temperature.

also with that of the two decomposed Raman bands in a -C:H films.

Absorption spectra of a -C:H films deposited on glass substrates were measured and plotted in Fig. 7 using the relation²⁶

$$(\alpha E)^{1/2} \propto (E - E_{\text{opt}}), \quad (2)$$

where α and E are the absorption coefficient and energy, respectively. Extrapolation of the straight line to the abscissa gives the optical gap E_{opt} . The values of the optical gap for various films change from 1.2 to 1.5 eV. The optical gaps of a -C:H films decrease with an increase in the substrate temperature. The absorptions associated with the π - π^* transition in π -bonded materials are found between 10 000 and 45 000 cm^{-1} (for example, at about 16 000 and 43 000 cm^{-1} for transpolyacetylene and benzene, respectively).⁶ As seen in Fig. 7, the absorptions around 20 000 cm^{-1} increase with an increase in the substrate temperature.

Figure 8 displays Raman spectra of a -C:H films excited by an excitation energy near 20 000 cm^{-1} . The disorder band becomes stronger with an increase in the substrate temperature. Comparing Figs. 7 and 8, the disorder band becomes stronger with an increase of the absorption due to the π - π^* transition in the $(\alpha E)^{1/2}$ spectra.

The electron-energy-loss spectra (EELS) of a -C:H films

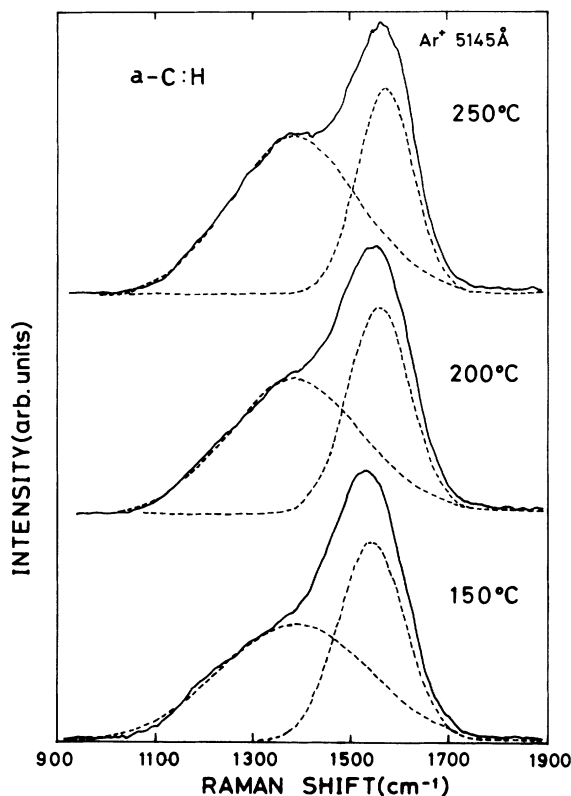


FIG. 8. The Raman spectra of a -C:H films excited at the 5145-Å line. The Raman spectra were given after subtracting the background due to luminescence. The two Raman bands decomposed with Gaussian line shapes are also shown in Fig. 8.

are shown in Fig. 9. Two peaks are seen, a weak one of approximately 6.7 eV due to plasma oscillations of π electrons, and a strong peak from $(\pi + \sigma)$ valence electrons at about 25 eV.¹¹ The intensity of the weak peak, due to the π plasmon, increases with the increase in the substrate temperature. A comparison among EELS, $(\alpha E)^{1/2}$, and the Raman spectra confirms that the variation in the Raman spectra due to the excitation wavelength of the *a*-C:H films is the result of π - π^* resonant Raman scattering from sp^2 carbon clusters having various sizes. A similar resonant Raman scattering from sp^2 carbon clusters having various sizes has also been observed in such polyene structures as polyacetylene.²⁷

In Fig. 6, the dependence of the frequencies of the two Raman bands on the excitation wavelength for GC implanted heavily with a fluence of 1×10^{16} B ions/cm² coincides well with that of the two Raman bands in *a*-C:H films. The coincidence between the variations in the Raman spectra due to the wavelength of the excitation energy shows that π - π^* resonant Raman scattering from various-sized sp^2 carbon clusters occurs in the heavily implanted GC.

IV. CONCLUSION

Raman spectra of the B ion-implanted GC and *a*-C:H films have been measured as a function of polarization direction of the scattered light and excitation wavelength. Raman bands of GC implanted heavily with a fluence of more than 5×10^{15} B ions/cm² and *a*-C:H films show a

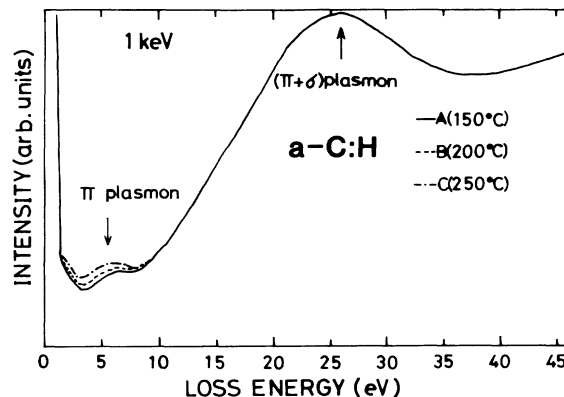


FIG. 9. The electron-energy-loss spectra of *a*-C:H films.

frequency-independent depolarization ratio, suggesting the existence of sp^2 carbon clusters. It was found that the Raman spectral profile for the heavily implanted GC varied with the excitation wavelength. From the similarity between the variation of the Raman spectra with excitation wavelength for the heavily implanted GC and *a*-C:H films, it is suggested that the spectral variation observed for the heavily implanted GC was caused by π - π^* resonant Raman scattering from various-sized sp^2 carbon clusters. These results support the validity of the molecularlike cluster model for the microstructures of the heavily implanted GC and the *a*-C:H films.

*Present address: Film and Film Products, Research Laboratories, Toray Industries, Inc., Sonoyama 3-3-7, Otsu, Shiga 520, Japan.

¹R. J. Nemanich and S. A. Solin, *Phys. Rev. B* **20**, 392 (1979).

²F. Tuinstra and J. L. Koenig, *J. Chem. Phys.* **53**, 1126 (1970).

³M. H. Brodsky, *Light Scattering in Solids I* (Springer-Verlag, Berlin, 1975), p. 205.

⁴P. Koidl, Ch. Wild, B. Dischler, J. Wagner, and M. Ramsteiner, *Mater. Sci. Forum* **52-53**, 41 (1989).

⁵M. Yoshikawa, G. Katagiri, H. Ishida, A. Ishitani, and T. Akamatsu, *Appl. Phys. Lett.* **52**, 1639 (1988).

⁶M. Yoshikawa, G. Katagiri, H. Ishida, A. Ishitani, and T. Akamatsu, *J. Appl. Phys.* **64**, 6464 (1988).

⁷M. A. Tamor, J. A. Haire, C. H. Wu, and K. C. Hass, *Appl. Phys. Lett.* **54**, 123 (1989).

⁸M. Yoshikawa, *Mater. Sci. Forum* **52-53**, 365 (1989).

⁹J. Wagner, M. Ramsteiner, Ch. Wild, and P. Koidl, *Phys. Rev. B* **40**, 1817 (1989).

¹⁰B. Dischler, A. Bubenzer, and P. Koidl, *Appl. Phys. Lett.* **42**, 636 (1983).

¹¹J. Fink, T. Müller-Heinzerling, J. Pflünger, A. Bubenzer, P. Koidl, and G. Crecelius, *Solid State Commun.* **47**, 687 (1983).

¹²N. Savvides, *J. Appl. Phys.* **58**, 518 (1985).

¹³N. Savvides, *J. Appl. Phys.* **59**, 4133 (1986).

¹⁴N. Wada and S. A. Solin, *Physica*, **105B**, 353 (1981).

¹⁵J. Robertson and E. P. O'Reilly, *Phys. Rev. B* **35**, 2946 (1987).

¹⁶B. S. Elman, M. S. Dresselhaus, G. Dresselhaus, E. W. Maby, and H. Mazurek, *Phys. Rev. B* **24**, 1027 (1981).

¹⁷R. Loudon, *Adv. Phys.* **13**, 423 (1964).

¹⁸H. W. Schrotter, *Raman Spectroscopy* (Plenum, New York, 1970), p. 69.

¹⁹T. Okada, H. Sasaki, S. Hayashi, S. S. Kim, and K. Yamamoto, *Solid State Commun.* **61**, 671 (1987).

²⁰R. O. Dillon, J. A. Woollam, and V. Katkanant, *Phys. Rev. B* **29**, 3482 (1984).

²¹Z. Iqbal and S. Vepřek, *J. Phys. C* **15**, 377 (1982).

²²M. A. Tamor, J. A. Haire, C. H. Wu, and K. C. Hass, *Appl. Phys. Lett.* **54**, 123 (1989).

²³J. Robertson, in *Diamond and Diamond-like Carbon Films*, edited by J. C. Angus *et al.* (Plenum, New York, 1991), p.1.

²⁴F. Li and J. S. Lannin, *Phys. Rev. Lett.* **65**, 1905 (1990).

²⁵J. Robertson, *Adv. Phys.* **35**, 317 (1986).

²⁶B. Dischler, A. Bubenzer, and P. Koidl, *Appl. Phys. Lett.* **42**, 636 (1983).

²⁷I. Harada, Y. Furukawa, M. Tasumi, H. Shirakawa, and S. Ikeda, *J. Chem. Phys.* **73**, 4746 (1980).